中華民國力學學會

第十六屆全國力學會議論文集(二)

中華民國基隆市　　八十一年十二月

Proceedings of the 16th National Conference

on Theoretical and Applied Mechanics

Soceity of Theoretical and Applied Mechanics of the Republic of China

Keelung, Taiwan, R.O.C. December 1992

CHIH-KAO MA （馬志高）.....735
STUDY ON THE CHARACTERISTICS OF STRUCTURAL OPTIMIZATION IN A FUZZY ENVIRONMENT
C.F.HUNG （洪振發）、**H.C.KUO** （郭信川）.....743
OPTIMAL PLACEMENT OF PIEZOELECTRIC ACTUATORS FOR ACTIVE STRUCTURAL ACOUSTIC CONTROL
BOR-TSUEN WANG （王栢村）、**RICARDO A. BURDISSO**、**CHRIS R.FULLER**.....751
夾具延伸台結構最佳化分析
楊宗文、陳春成、喬國鎮.....759
對偶積分表示式在剪力梁漫散振動的應用
葉超雄、洪宏基、陳正宗.....767
反應器壓力容器之可靠度分析
林棋瑋、吳文方、張順庭.....775

土壤力學 （一）

螺線一直線組合之破壞面的砂土主動土壓力係數
祝錫智.....783
側向變形對壓密試驗結果的影響
許澤善、鍾彩俊.....791
臺北盆地基二區粉質粘土之非線性應力應變關係
許曉峰、李崇正.....797
生石灰樁對軟弱黏性土壤工程性質之改良效果
張惠文、洪明瑞、MASARU ARAISHI.....805
樁材表面性質對樁土間摩擦行爲之影響
廖新興、林杏性、張惠文.....813
土壤性質受汚染影響之研究
張天祥、陳俶季.....821

土壤力學 （二）

顆粒級配效應對粒狀土壤微觀組構之影響
簡連貴、李建中、劉崑安.....829
表面波分散曲線的影響因素
康裕明.....837
層狀土壤內波數之數值解

中華民國第十六屆全國力學會議
THE SIXTEENTH NATIONAL CONFERENCE ON THEORETICAL AND APPLIED MECHANICS, KEELUNG, TAIWAN, R.O.C.

December 11-12, 1992

OPTIMAL PLACEMENT OF PIEZOELECTRIC ACTUATORS FOR ACTIVE STRUCTURAL ACOUSTIC CONTROL

Bor-Tsuen Wang

Department of Mechanical Engineering
National Pingtung Polytechnic Institute
Pingtung,Taiwan91207,R.O.C.

Ricardo A.Burdisso
Chris R.Fuller

Vibration and Acoustics Laboratories
Department of Mechanical Engineering
Virginia Polytechnic Institute and State University
Blacksburg,Virginia 24061,U.S.A.

ABSTRACT

This paper presents a general formulation of the optimization problem for the placement and sizing of piezoelectric actuators in adaptive LMS control systems. The selection of objective function, design variables and physical constraints are separately discussed. A case study for the optimal placement of multiple fixed size piezoelectric actuators in sound radiation control is presented. A solution strategy is proposed to calculate the applied voltages to piezoelectric actuators with the use of linear quadratic optimal control theory. The location of piezoelectric actuators is then determined by minimizing the objective function, which is defined as the sum of the mean square sound pressure measured by a number of error microphones. The optimal location of piezoelectric actuators for sound radiation control is determined and shown to be dependent on the excitation frequency. Particularly, the optimal placement of multiple piezoelectric actuators for on-resonance and off-resonance excitation is presented. Results show the optimally located piezoelectric actuators perform far better sound radiation control than arbitrarily selected ones. This work leads to a design methodology for adaptive or intelligent material systems with highly integrated actuators and sensors. The optimization procedure also leads to a reduction in the number of control transducers.

INTRODUCTION

Piezoelectric actuators haveHxeen widely used in structural sound and vibration control. Wang and Rogers (1991a, 1991b) presented the theoretical analysis of the mechanics of piezoelectric actuators, and Wang et al. (1991) demonstrated their potential as transducers in structural sound control. However, the proper selection of number and location of piezoelectric actuators is critical to efficiently control structural sound radiation. Therefore, the determination of the optimal placement and number of piezoelectric actuators in sound radiation control is an important and interesting issue.

Previous works, however, on optimal placement of actuators are mostly concerned with vibration control and particularly for feedback control system with the use of traditional force transducers, such as point force shakers, (Norris and Skelton, 1989; Chang and Soong, 1980; Hamidi and Juang, 1981; Juang and Rodriguez, 1979). For state feedback control, a state space equation is first constructed to represent the system model, and a performance index, which is a quadratic form in the state and control effort, can then be defined. Finally, the optimal location is to be determined by minimizing the performance index. Only a few literatures deal with the optimal location of distributed actuators, which are widely used in conjunction with so called "smart" structures. Jia (1990) studied the optimal position of piezoelectric actuators for beam vibration control by adopting the independent modal space control approach (IMSC). Jia showed that the optimal location and size of piezoelectric actuators can be found by minimizing an objective function which can be either the structural response, control effort, residual response, spillover effect or combinations of all/any of these variables. However, Jia's work is limited to consider only one-dimensional vibration control.

Adaptive feedforward control, on the other hand, has been adopted for structural sound radiation control in recent years (Gibbs and Fuller, 1990; Burdisso and Fuller, 1990; Simpson et al., 1989). Hxe control algorithm is flexible, because it is not as crucial as feedback approaches to accurately model the system response. The adaptive feedforward controller can learn the system parameters by itself and converge to the optimal solution using various "training" approaches. However, little work has been discussed on the optimal placement of actuators, particularly distributed in nature, for feedforward control. This paper is thus concerned with the formulation of the optimization problem for the placement of piezoelectric actuators in feedforward control systems, in particular for the ASAC technique.

In this paper, a general formulation for the optimal placement of piezoelectric actuators in a feedforward control approach is first presented and then applied to a typical sound radiation control system using piezoelectric actuators and microphone sensors. A baffled, simply-supported, rectangular plate as shown in Figure 1 is considered as an idealized system. The plate is harmonically excited by a primary source (point force), and piezoelectric actuators are applied to control the plate vibration in order to reduce the associated sound radiation. The objective here is to determine the optimal location of piezoelectric actuators such that the sound pressure measured from the error microphones can be most efficiently reduced (i.e., with lowest actuator power and/or number of actuators). A solution strategy is proposed to calculate the applied voltages to piezoelectric actuators with the use of linear quadratic optimal control theory (Wang, 1991), The location of the piezoelectric actuator(s) is then determined by minimizing the objective function, which is defined as the sum of the mean square sound pressure measured by a number of error microphones. The optimal locations for multiple piezoelectric actuators, up to three, were considered. The results show that the optimally placed actuators achieve a far better reduction of sound radiation than actuators whose positions are arbitrarily chosen.

MATHEMATICAL FORMULATION FOR OPTIMIZATION PROBLEM

Design Variables

As shown in Figure 2, the optimal placement of the j-th piezoelectric actuator located inside the boundaries of the plate can contain five variables, $\bar{x}_i$, $\bar{y}_i$, C_{xi} , C_{yi} and V_i . The variables C_{xi} and C_{yi} denote the size of the i-th piezoelectric actuator, while $\bar{x}_i$ and $\bar{y}_i$ denote the central location of the actuator, and V_i is the applied voltage to the piezoelectric actuator. If the primary source is known, and piezoelectric actuators are used as control sources, then the total radiated sound pressure can be shown as follow:

$$P_t = P_t(\bar{x}_i, \bar{y}_i, C_{xi}, C_{yi}, V_i) \quad i = 1,\ldots,N_c \tag{1}$$

The complete derivation of p_t is shown in (Wang, 1991) and omitted here. As discussed from previous works (Wang et al., 1991), V_i can be calculated from the linear quadratic optimal control theory (LQOCT). The total radiated sound pressure can then be written as follow:

$$P_t = P_t(\bar{x}_i, \bar{y}_i, C_{xi} C_{yi}, V_i(\bar{x}_i, \bar{y}_i, C_{xi}, C_{yi})) \quad i = 1,\ldots,N_c \tag{2}$$

However, if the size of piezoelectric actuators was first fixed, then the total radiated sound pressure becomes

$$p_t = p_t(\bar{x}_i, \bar{y}_i, v_i(\bar{x}_i, \bar{y}_i)) \quad i = 1,\ldots,N_c \tag{3}$$

The design variables, $\bar{x}_i$, $\bar{y}_i$, C_{xi} , C_{yi} and V_i , can be properly selected based upon the concern of the size, location or both of the piezoelectric actuator and the control effort (i.e., the voltages or power required for piezoelectric actuators).

Objective Function

There are various choices for the objective function. Wang et al. (1991) chose the integral of the square of radiated sound pressure over a hemisphere of the radiating field, as the cost function. However, such a cost function, in practice, is not useful. Wang and Fuller (1991) constructed a cost function which is the sum of the mean square radiated sound pressures measured by a limited number of microphones, The consideration of the above two types of objective functions is particular of interest in sound radiation control. Since the sound radiation is strongly coupled with the structural vibration, the objective function may also be chosen as the sum of the mean square plate acceleration measured by a limited number of accelerometers or the integral of the square of the plate acceleration over the vibrating surface. The possible candidates of the objective function used in sound radiation control can be as follows:

(1) Distributed pressure sensors

$$\Phi_p = \frac{1}{R^2}\int_s |p_t|^2 ds = \int_0^{2\pi}\int_0^{\frac{\pi}{2}} |p_t|^2 \sin\theta d\theta d\phi \tag{4}$$

(2) Discrete pressure sensors

$$\Psi_p = \sum_{i=1}^{N_{mike}} |p_{t_i}(R_i, \theta_i, \phi_i)|^2 \tag{5}$$

(3) Distributed accelerometer sensors

$$\Phi_w = \int_A |\ddot{w}_t|^2 dA = \int_0^{L_y}\int_0^{L_x} |\ddot{w}_t|^2 dx dy \tag{6}$$

(4) Discrete accelerometer sensors

$$\Psi_w = \sum_{i=1}^{N_{acc}} |\ddot{w}_{t_i}(x_i, y_i)|^2 \tag{7}$$

where N_{mike} and N_{acc} are the number of microphones and accelerometers respectively. It is noted that Φ_p and Φ_w are measured by ideal distributed sensors,which may not be practical in reality; however, Φ_p and Φ_w represent the power of sound radiation or energy density of out-of-plane structural vibration. They can be used as an index of control effectiveness. For practical applications, Ψ_p and Ψ_w are the alternative options. A reasonable number and location of sensors shall be selected to reflect the actual system response, such that an optimal solution can be found without losing the global nature of the problem. In effect, the discrete sensors should approach a form of numerical integration of the objective function associated with the distributed sensors to be truly global.

Design Constraints

The design constraints have to be specified to confine the design variables within a reasonable range. These design constraints are necessary for providing a reasonable result by maintaining the rectangular shape of piezoelectric actuators, locating actuators inside the plate boundaries, avoiding overlapping between actuators, and operating actuators within the working voltage range. It is noted that the constraint set (iii) for avoiding overlapping is conceptually sketched in Figure 3. For the rectangular-shaped piezoelectric actuators as shown in Figure 3, the constraint sets are listed as follows:

(i) To maintain the piezoelectric actuator a rectangular shape:

$$\begin{aligned} 0 < C_{x_i} &\le L_x/2 \\ 0 < C_{y_i} &\le L_y/2 \end{aligned} \tag{8}$$

(ii) To maintain the piezoelectric actuator inside of the plate:

$$\begin{aligned} \bar{x}_i - C_x/2 &\ge 0 \\ \bar{x}_i + C_x/2 &\le L_x \\ \bar{y}_i - C_y/2 &\ge 0 \\ \bar{y}_i + C_y/2 &\le L_y \end{aligned} \tag{9}$$

(iii) To avoid overlapping between piezoelectric actuators:

$$\begin{aligned} &\bar{x}_{i+1} - \bar{x}_i > 0 \\ &\bar{y}_{i+1} - \bar{y}_i > 0 \\ &[(\bar{x}_{i+1} - \bar{x}_i)^2 + (\bar{y}_{i+1} - \bar{y}_i)^2]^{1/2} \\ &- \frac{1}{2}[(C_{xi}^2 + C_{yi}^2)^{1/2} + (C_{x_{i+1}}^2 + C_{y_{i+1}}^2)^{1/2}] > 0 \end{aligned} \tag{10}$$

(iv) To specify the working range of piezoelectric actuators;

$$|V_i| \le 150(volt\ p\text{-}p) \tag{11}$$

Note that the control power to the actuators is not an optimization variable. However, constraint (iv) ensures that the piezoelectric actuator is within a working range.

APPLICATION TO OPTIMAL PLACEMENT OF PIEZOELECTRIC ACTUATORS

For a simple application of the previous theoretical formulation to sound radiation control, the size of piezoelectric actuators is assumed fixed, i.e., C_{xi} = C_{yi} = constant. The applied voltage to the i-th piezoelectric actuator, V_i , can be calculated from LQOCT, (Wang,

1991). Only the optimal location of piezoelectric actuators, $\bar{x}_i$ and $\bar{y}_i$, will be determined. The objective function is chosen as the sum of the mean square sound pressure measured by a number of microphones in the far-field. Therefore, the optimization problem can be written as:

Objective function:

$$\Psi_p = \Psi_p(\bar{x}_i, \bar{y}_i, V_i(\bar{x}_i, \bar{y}_i)) = \sum_{j=1}^{N_{mike}} |P_{t_j}(R_j, \theta_j, \phi_j)|^2, \quad i=1,\ldots,N_c \tag{12}$$

design variables:

$$(\bar{x}_i, \bar{y}_i) \quad i=1,\ldots,N_c \tag{13}$$

design constraints:
constraint set (ii), (iii) and (iv), as shown in Equations (9)-(11).

The design variables are to be determined by minimizing the objective function subjected to a set of design constraints. Now, a suitable optimization algorithm must be adopted to solve the optimal solution.

OPTIMIZATION ALGORITHM

An IMSL subroutine N0ONF (IMSL, 1989), for solving a general nonlinear programming problem using the successive quadratic programming algorithm and a finite difference gradient technique, was adopted to calculate the optimal solution. The algorithm requires a high accuracy arithmetic in estimating the gradient. The central finite difference method was then applied to approximate the gradient by adopting the IMSL CDGRD subroutine (IMSL, 1989).

Solution Strategy

To solve the above optimization problem, a solution strategy was developed. The flow chart of solution strategy is shown in Figure 3. The procedure to solve the problem is first to set up the initial guess of the optimal central location of the i-th actuator, $(\bar{x}_i)_k$, $(\bar{y}_i)_k$, where k denote the number of iteration. The following steps are then proceeded:

1. utilize the linear quadratic optimal control theory (LQOCT) (Wang, 1991) to obtain the applied voltages, $(V_i)_k$, to actuators at the current location, $(\bar{x}_i)_k$, $(\bar{y}_i)_k$.
2. evaluate the objective function and constraints at the current location, $(\bar{x}_i)_k$, $(\bar{y}_i)_k$.
3. evaluate the gradients of the objective function and constraints at the current location, $(\bar{x}_i)_k$, $(\bar{y}_i)_k$.
4. employ an optimization algorithm, N0ONF, to update the optimal location, $(\bar{x}_i)_{k+1}$, $(\bar{y}_i)_{k+1}$.
5. stop the procedure if the results pass the accuracy test; otherwise, update the current optimal location of actuators and repeat the above steps.

It is noted that the design variables, the central location of piezoelectric actuators $(\bar{x}_i, \bar{y}_i)$, was normalized by the plate length and width (L_x, L_y) respectively such that the design variables will be relocated between zero and one. This normalization process will benefit the solution process of the optimization problem.

LQOCT for Solving Applied Voltages to Actuators

Lester and Fuller (1990) presented an optimization algorithm to obtain the minimum for a linear quadratic function. Wang et al. (1991) had shown the use of linear quadratic optimal control theory (LQOCT) to determine the applied voltages to minimize the selected objective function which is quadratic. Here, the LQOCT is adopted to solve the voltages independently. One of the advantages is that the optimal voltages can be always determined whenever the location of actuators is known. The other reason to evaluate the optimal voltage separately because the order of voltage and the central location of piezoelectric actuator is not consistent arithmetically, even after the normalization process. Hence, upon the consideration of numerical difficulty and the number of design variables, it is beneficial to obtain the optimal voltage using LQOCT separately from solving the optimization problem.

ANALYTICAL RESULTS

Table 1 shows the physical properties of the simply-supported plate used for the following simulations. The structural disturbance was assumed to be a point force with magnitude of F_1 =1N and located at x_{f1} =0.08m, y_{f1} =0.08m. Nine error microphone sensors, whose locations are tabulated in Table 2 and shown in Figure 4, were used; therefore, the objective function defined in Equation (12), which is the sum of mean square measured pressure, can be constructed. The reason to choose this number of microphones is based on the consideration of computing time and a reasonable approximation to the continuous integral of pressure over the complete radiation hemisphere. Too few microphones will not reveal the actual system global radiation response. On the other hand, too many microphones will require excessive computing effort to solve the optimization problem. The microphones located in the far-field are arranged five in a row across the central line of the plate in both the x- and y-directions, as shown in Figure 4. The size of piezoelectric actuators is fixed, C_{xi} =0.06 m and C_{yi} =0.04m. The location and applied voltages of piezoelectric actuators are to be determined.

Sub-Region Search Method

The determination of the optimal location of piezoelectric actuators is dependent on the excitation frequency. A different excitation frequency will lead to a different optimal location. For a particular frequency of excitation, all of the plate modes can be excited; however, only the plate modes near the excitation frequency will contribute significantly to the plate response as well as the sound radiation. It is clear that if the plate was excited near the (1,1) mode, the plate response will be shown as a convex surface. Similar characteristic can be found for the objective function. If the plate was excited at 87 Hz near the (1,1) mode, and the central location of piezoelectric actuator was varied and moved around the plate, then the objective function and the applied voltage can be calculated from LQOCT and plotted as shown in Figure 5. Because the objective function is shown as a convex surface, an optimal location of the piezoelectric actuator can be always found to guarantee global minimum. It is also noted, from Figure 5, that high control voltages are required for the actuator located near the corner of the plate to achieve sound radiation control. The actuator having the minimum control effort is located at about the same position as the actuator having the minimum objective function.

Also shown in Figure 6, for an excitation frequency f = 357 Hz near the (3,1) mode, the objective function and the applied voltage reveal a shape cloHx to the (3,1) mode distribution. There are more than one minimum for the objective function; in fact, there is one local minimum at each division separated by nodal lines. This characteristic,

related to the plate mode shapes, is similar to what has been seen in Figure 5. If the actuator is located near the nodal line of the plate mode, then sound radiation control is not effective, at least for on-resonance excitation, because of high control voltage and small control authority.

Figure 7 shows the similar plots as Figures 5 and 6 except that the excitation frequency, f = 272 Hz, is between the (2,1) and (3,1) modes. One can see that those distributions become complex and results from combination of several plate modal responses. Again, there are multiple minima; this makes the optimization procedure to find a global minimum difficult. However, according to the characteristics shown in Figures 5 and 6, a sub-region search method, which comes from the nature of the objective function distribution similar to that of the plate mode shapes, can be proposed. This search technique is to subdivide the plate into several cells based on the nodal lines of the plate mode shapes, which are set up to be the bound of the locations for the actuators. In other words, in addition to the design constraints illustrated previously, the upper and lower bounds of the locations for actuators can also be specified according to the nodal lines associated with the plate mode shapes.

Optimal Location of One Actuator for Different Excitation

As discussed previously, the optimal location of piezoelectric actuators is dependent on the excitation frequency due to the variation of modal transfer function in frequencies. The optimal location of actuator has been of interest for many concerns. As discussed by Juang and Rodriguez (1979), to control a single mode of beam vibration, there are multiple optimal locations for one actuator in high-mode control. If several modes contribute to the response simultaneously, and only a few actuators are applied, then the optimal location will be much different from that for single mode control. The feedforward control approach adopted here is to minimize the objective function, which is the mean square of sound pressure measured by error microphones, and thus to control all of the modal contributions at the same time. Therefore, the optimal location and applied voltage of the actuator is solved under a compromise to eliminate the significant modal responses; however, this compromise will probably incur spillover to other higher modes, which do not radiate efficiently to the error microphones, causing an increase in plate response.

When one piezoelectric actuator was considered, the normalized optimal central location of the piezoelectric actuator and the applied voltage to the actuator are tabulated in Table 3 as well as the reduction of the objective function, radiated power and pressure modal amplitude. Table 3 is shown for different excitation frequencies varying from 87 Hz to 357 Hz, i.e., between the (1,1) and (3,1) modes. The underlined values are for on-resonance excitation, such as 87 Hz near the (1,1) mode, 190 Hz near the (2,1) mode and 357 Hz near the (3,1) mode. One can see that the optimal central location of the actuator is located at about one third of the plate length and width, in the left-bottom quadrant of the plate, i.e., the same quadrant where the point force disturbance is located. As the excitation frequency increases, the optimal central location of the actuator moves in the direction toward the corner of the plate. This can be understood by the realization that when the excitation frequency increases, the contribution of higher modes becomes significant, and thus the optimal location of the actuator is placed where it can couple into all higher mode responses. In applying one actuator, for example f = 87 Hz near the resonance of the (1,1) mode, the actuator attempt to control all of the significant radiating mode responses, including the (1,1) and (2,1) modes, instead of just the (1,1) mode. Therefore, the optimal location is determined under a compromise to eliminate the significant modes; however, as one can see in Table 17, there is spillover to higher modes, such as (3,1), (4,1) and (5,1) modes. This result indicates that the optimal location of single actuator is to eliminate the significant modal response near the excitation frequency; however, this will result in spillover to higher modes, which ultimately limit the amount of attenuation.

On the other hand, when the excitation frequency increases, for example f=357 Hz near the (3,1) mode excitation, the radiation from (3,1) mode is controlled as well as the (1,1) and (2,1) modes, but with less reduction. There is still spillover to the higher modes but less than at the lower frequency excitations. This can be explained that the (1,1) and (2,1) modes, having high radiation efficiency can contribute a larger amount of sound radiation to the far-field, even though the (3,1) mode is dominant on the plate due to the excitation frequency. Therefore, the optimal location is determined from a result of compromise to efficiently eliminate the most significant radiating modes, i.e., the (1,1), (2,1) and (3,1) modes in this case. However, this effort causes the spillover to higher modes, such as (4,1) and (5,1) modes, which have lower radiation efficiency (Wallace, 1972). It is also noted, from Table 3, that for on-resonance excitation, the reduction of radiated power is generally larger, and the control effort (voltage) is higher than those cases for off-resonance excitation. This result is due to the fact that modes on resonance always contributes considerably more to the modal response and thus require more control effort.

Optimal Location of Multiple Actuators for Different Excitation Frequencies

On-Resonance Excitation, f=357 Hz, Near (3,1) Resonant Mode

Table 4 shows the optimal central location and applied voltages of piezoelectric actuators as well as the reduction of objective function and radiated power for an excitation frequency of f = 357 Hz. As one can see, although the reduction of objective function increases when more actuators are applied, the amount of attenuation of radiated power is not always increased. This means the optimization algorithm does work to find a better solution. However, the minimization of the objective function, which is the sum of mean square pressures measured by error microphones, will not guarantee the reduction of radiated power due to the spillover of sound pressure to other locations than the position of error microphones. In term of the attenuation of radiated power, to properly locate one actuator in controlling sound radiation is more effective than to use two or three actuators when a set of microphones are used as error sensors, as it reduces unnecessary spillover.

Figure 8 shows the radiation directivity pattern for the excitation frequency f = 357 Hz. The point force disturbance input and piezoelectric actuator patches are sketched to scale on the top of Figure 8. The disturbance response denoted by a solid line indicates a monopole like response, but is nonuniform, and evidently shows the existence of the (3,1) mode and a significant (1,1) modal contribution. The optimal location of one actuator is at the left-bottom quadrant of the plate similar to the primary source. The residual pressure field is shown to be a combination of the (3,1) and (1,1) modes.

For two-actuator control as shown on the top of Figure 8, the first optimally located actuator is somewhat near the optimal location for one-actuator control, and the second one is located at the up-right quadrant of the plate near the central line. As shown in Table 4, the reduction of objective function is increased, but the reduction of radiated power is decreased. A result such as this implies that more error microphones need to be used, due to spillover effects to unobserved radiation points. Nevertheless, the sound pressure level along the central line of the plate in both x- and y-direction is less than that using one actuator and exhibits a combination of the (4,1) and (1,1) modes. It can be seen that there are dips at θ-0° , 75° for ϕ-0° , and 75° for ϕ-180° . where the error microphones are located. For three-actuator control, the optimal location of the first two actuators are close to those of two-actuator control, and the third one is located at the bottom-right quadrant of the plate. Again, the objective function has been further minimized. As shown in Figure 8 the dips at θ-0°,75° for ϕ-0° and 75° for ϕ-180° are enhanced, but the reduction of radiated power has not increased.

An interesting feature can be observed from the above results indicating that a one-by-one search method may be used to solve for the location of the successive actuator. The idea is first to find an optimal location for one-actuator control, and then to find a second optimal location for two-actuator control having the same location for the first actuator, and so on. With this searching technique, the computing time can be largely reduced, since it would cost less to optimize a reduced-parameter problem than a full-parameter problem. This method was tried; however, the results were not encouraging, since the selected objective function cannot be attenuated further due to numerical difficulty (even though double precision number was used in program), while an additional actuator was considered. The authors believe that if the objective function is reconstructed as the radiated power rather than the mean square pressure, the one-by-one search method would be appropriate and can reduce significant computing effort for multiple actuator control. Also, it appears that each actuator is optimally configured for separate modes, since their locations stay the same. Hence, an independent optimization procedure for each mode and its associated radiation might be tried.

Also shown in Figure 8 is an arbitrary selection of multiple actuators located at one sixth of the plate length or width (denoted lab arrangement). This arrangement is assigned to control the low modal number excitation based upon the nature of the plate mode shapes and was used in companion experiments (Clark and Fuller, 1990). The results show that optimally configured one-, two- or three-actuator control is superior to the arbitrarily chosen actuators for the on-resonance excitation in terms of both objective function and radiated power.

Figure 9 shows the plate displacement distribution corresponding to the cases of Figure 8. The solid line depicts the disturbance response and reveals that the (3,1) mode is dominant. With control, the plate displacement has been reduced globally and exhibits a more complex pattern, and the (3,1) mode has been attenuated considerably. Further comments on the behavior are as in previous section.

Off-Resonance Excitation, f=272 Hz, Between (2,1) and (3,1) Resonant

Table 5 shows the optimal central location and applied voltages of piezoelectric actuators as well as the reduction of objective function and radiated power for an excitation frequency f = 272 Hz between the (2,1) and (3,1) modes. The control effort (i.e., the control voltages) is not necessary smaller than that for on-resonance excitation, unlike the previous observation for one-actuator control. In fact, either one of the actuators may require extremely high control voltages; however, others may simultaneously need only a small voltage. The optimal location and required control voltages for multiple actuators are determined in a way not only to suppress the disturbance response but also to reduce the interactive spillover effects due to actuators themselves.

Figures 10 and 11 show the radiation directivity pattern and the plate displacement distribution respectively corresponding to the case in Table 5 for the off-resonance excitation. The optimal location of piezoelectric actuators, sketched on the top of Figure 10, are very similar to that of the on-resonance excitation. From Figure 10, the primary radiated sound denoted by a solid line shows a small dip at $\theta=0°$ indicating the strong response of the (2,1) mode. In applying one actuator, the residual response shows a combination of the (3,1) and (1,1) modes, and there are no dips at any location of the error microphones. In applying two and three actuator, the residual response reveals a more complex pattern similar to the (4,1) and (5,1) modes respectively. Dips can now be seen located at the error microphone locations. It is again shown that increased actuators can further attenuate the pressures at error microphone position; however, the overall radiated power is not necessarily reduced, because of spillovers in sound pressure into other locations than the position of the error microphones.

The plate displacement distribution for the case of disturbance, as shown in Figure 11, exhibits the (2,1) mode characteristic shape. With control, the residual plate response reveals a more complex pattern and is not attenuated globally as what was seen in Figure 11 for resonance excitation. This phenomenon is referred to as "modal restructuring" for the off-resonance excitation and "modal suppression" for the on-resonance excitation (Fuller, Hansen and Snyder, 1990).

COMPUTING TIME ANALYSIS

In an optimization procedure, to find the gradient of objective function is generally the most difficult and the most CPU time consuming task. Table 6 shows the percentage of CPU time consumed for each step in the optimization procedure. It takes about 20%. of CPU time for steps 1 and 2, i.e., the evaluation of objective function and the applied voltages to actuators, and over 70% (up to 90% for three actuators) of CPU time for step 3, i.e., the evaluation of the gradients of the objective function and constraints in the optimization procedure. However, it takes only a small percentage of time for step 4 in calculating the update actuator's location in the optimization subroutine. In order to efficiently solve the optimization problem, it is necessary to do a sensitivity analysis. For future work, it could be beneficial to apply an analytical or semi-analytical method rather than finite difference method to evaluate the gradients so that CPU time can be reduced for solving the optimization problem. Furthermore, the acoustic radiated power could also be considered as objective function to solve the optimal location of piezoelectric actuators.

SUMMARY

This paper has presented the mathematical formulation for the optimization problem of the placement of piezoelectric actuators in a feedforward control implementation of ASAC. The analysis is applied to an example problem to obtain preliminary information on how the optimization procedure performs. Four different forms of objective functions, which are differentiated by discrete or distributed and by vibrational or pressure sensor, are discussed for sound radiation control. An objective function, which is constructed based on the use of a number of discrete pressure sensors, is applied to the example of sound radiation control. Some significant observations may be summarized as follows:

1. Different excitation frequencies will result in different optimal locations of piezoelectric actuators.

2. The optimally located piezoelectric actuators can provide a large amount of reduction of sound radiated power and are seen to perform better than arbitrarily chosen locations. To properly locate one piezoelectric actuator generally gives higher reduction of radiated acoustic power than to use two or three actuators for the selected objective function which is the sum of mean square sound pressure measured by a limited number of microphones. This is due to control spillover resulting from driving down the error signals at all error microphones. An alternative would be to limit the attainable attenuation achieved at each error microphone or use the total radiated power as the objective function.

3. A computing time analysis shows that the evaluation of the gradients of the objective function and constraints consumes most of the CPU time. Sensitivity analysis, which can be used to analytically or semi- analytically evaluate the gradients, is required for future research.

4. This work, which lays out the theory for optimal location of piezoelectric actuators, will be the basis for design of "smart" structures for ASAC with distributed actuators and sensors.

REFERENCES

Burdisso, R. A., and C. R. Fuller, 1992, "Theory of Feed-Forward Controlled System Eigenproperties," ***Journal of Sound and Vibration***, **153**(3), pp.437-451.

Chang, M. I. J., and T. T. Soong, 1980, "Optimal Controller Placement in Modal Control of Complex Systems," ***Journal of Mathematical Analysis and Applications***, **75**, pp. 340-358.

Clark, R. L., and C. R. Fuller, 1992, "Modal Sensing of Efficient Acoustic Radiation with PVDF Distributed Sensors in Active Structural Acoustic Control Approaches," ***Journal of the Acoustical Society of American***, **91**(6), pp. 3321-3329.

Fuller, C. R., C. H. Hansen, and S. D. Snyder, 1991, "Active Control of Sound Radiation From a Vibrating Rectangular Panel by sound sources and vibration inputs: An Experimental Comparison," ***Journal of Sound and Vibration***, **145**(2), pp.195-215.

Gibbs, G. P., and C. R. Fuller, 1992, "Experiments on Active Control of Vibrational Power Flow Using Piezoceramic Actuators and Sensors," ***AIAA Journal***, **30**(2), pp. 457-463.

Hamidi, M., and J.-N. Juang, 1981, "Optimal Control and Controller Location for Distributed Parameter Elastic Systems," ***Proceedings of the 20th IEEE conference on Decision and Control***, pp. 502-506.

IMSL, 1989, ***IMSL Math /Library***, IMSL Problem-Solving System Software System.

Jia, J., 1990, "Optimization of Piezoelectric Actuator Designs in Vibration Control Systems," PhD Thesis, Department of Mechanical Engineering, VPI&SU, Blacksburg, Virginia.

Juang, J.-N., and G. Rodriguez, 1979, "Formulations and Applications of Large Structure Actuator and Sensor Placements," ***Proceedings of the Second VPI&SU/AIAA Symposium on Dynamics and Control of Large Flexible Spacecraft***, Blacksburg, Virginia, June.

Lester, H. C., and C. R. Fuller, 1990, "Active Control of Propeller Induced Noise Fields Inside a Flexible Cylinder," ***AIAA Journal***, **28**(8), pp. 1374-1380.

Norris, G. A., and R. E. Skelton, 1989, "Selection of Dynamic Sensors and Actuators in the Control of Linear Systems," ***Journal of Dynamic Systems, Measurement, and Control***, **111**, September, pp. 389-397.

Simpson, M. A., T. M. Luong, C. R. Fuller, and J. D. Jones, 1992, "Full Scale Demonstration Tests of Cabin Noise Reduction Using Active Vibration Control," ***Journal of Aircraft***, **30**(3), pp. 624-630.

Wallace, C. E., 1972, "Radiation Resistance of a Rectangular Panel," ***Journal of Acoustical Society of America***, **51**, pp. 946-952.

Wang, B.-T., E. K. Dimitriadis, and C. R. Fuller, 1990, "Active Control of Structurally Radiated Noise Using Multiple Piezoelectric Actuators," ***AIAA Journal***, **29**(11), pp. 1802-1809.

Wang, B.-T., and C. R. Fuller, 1991, "Study of the Effect of Distributed or Discrete Pressure and Acceleration Sensors on Active Structural-Acoustic Control Systems," ***Proceedings of the Eight National Conference of the Chinese Society of Mechanical Engineering***, Taipei, Taiwan, R.O.C., pp. 1445-1454.

Wang, B.-T., and C. A. Rogers, 1991a, "Modeling of Finite-Length Spatially Distributed Induced strain Actuators for Laminate Beams and Plates," ***Journal of Intelligent Material Systems and Structures***, **2**(1), pp. 38-58.

Wang, B.-T., and C. A. Rogers, 1991b, "Laminate Plate Theory for Spatially Distributed Induced strain Actuators," ***Journal of Composite Materials***, **25**(4), pp. 433-452.

Wang, B.-T, 1991, "Active Control of Sound Transmission/Radiation From Elastic Plates Using Multiple Piezoelectric Actuators," PhD Thesis, VPI&SU, Blacksburg, Virginia.

Table 1. Plate specification

$E = 207 \times 10^9$ (N/m^2)	$\nu = 0.292$
ρ_p =7870 (kg/m^3)	h = 1.5875 (mm)
L_x = 0.38(m)	L_y = 0.30 (m)

Table 2. Location of error microphones

the i-th microphone	(R,θ,ϕ)
1	(1.8,75°,180°)
2	(1.8,45°,180°)
3	(1.8,0°,0°)
4	(1.8,45°,0°)
5	(1.8,75°,0°)
6	(1.8,75°,90°)
7	(1.8,45°,90°)
8	(1.8,45°,270°)
9	(1.8,75°,270°)

Table 3. Results for one actuator with different excitation frequencies

excitation frequency	normalized optimal central location of actuator		optimal voltage (Volt)	reduction of objective function	reduction of radiated power	reduction of pressure modal amplitude (dB)				
f(Hz)	$\bar{x}/L_x$	$\bar{y}/L_y$	V	Ψ_p (dB)	Φ_p (dB)	(1,1)	(2,1)	(3,1)	(4,1)	(5,1)
87	0.3456	0.3933	51.15	171.22	101.51	56.55	12.61	-2.47	-18.94	-27.62
100	0.3442	0.3919	49.89	147.27	59.61	30.94	17.55	-3.53	-18.54	-25.50
120	0.3413	0.3892	47.73	134.37	61.10	22.34	15.54	-1.58	-18.10	-27.45
140	0.3378	0.3861	45.37	128.43	53.33	17.69	18.36	-0.88	-17.63	-27.31
165	0.3324	0.3813	42.26	120.65	46.96	13.87	24.55	0.16	-16.77	-25.24
190	0.3255	0.3757	39.13	138.03	65.11	11.17	50.18	1.47	-15.74	-26.82
220	0.3150	0.3679	35.60	111.69	38.47	8.83	22.61	3.45	-14.52	-26.32
245	0.3043	0.3609	33.08	119.53	46.54	7.41	18.04	5.60	-12.66	-25.83
270	0.2920	0.3541	31.11	99.02	34.11	6.36	15.61	8.46	-10.76	-25.13
300	0.2765	0.3477	29.55	99.69	26.84	5.50	14.02	13.44	-7.94	-23.99
330	0.2631	0.3456	28.67	100.46	29.91	4.99	13.27	21.63	-4.74	-22.68
357	0.2548	0.3416	53.34	148.75	78.26	4.62	12.51	70.28	-1.22	-21.23

Table 4. On-resonance excitation, f=357 (Hz), near (3,1) mode

case	the i-th actuator	optimal location $\bar{x}/L_x$	$\bar{y}/L_y$	optimal voltage V_i (volt)	reduction of objective function,(dB)	reduction of radiated power,(dB)
one actuator	(1)	0.2548	0.3416	53.34	148.75	78.26
two actuators	(1)	0.2511	0.2852	100.54	189.06	6.70
	(2)	0.5504	0.6143	27.97		
three actuators	(1)	0.2499	0.2846	56.65	192.78	66.56
	(2)	0.5419	0.6052	50.61		
	(3)	0.8223	0.2198	61.09		
three actuators (Lab)	(1)	0.167	0.5	24.11	61.60	60.28
	(2)	0.5	0.833	25.73		
	(3)	0.833	0.167	10.78		

Table 5. Off-resonance excitation, f=272 (Hz), between (2,1) and (3,1) modes

case	the i-th actuator	optimal location $\bar{x}/L_x$	$\bar{y}/L_y$	optimal voltage V_i (volt)	reduction of objective function,(dB)	reduction of radiated power,(dB)
one actuator	(1)	0.2945	0.3533	59.68	104.73	34.66
two actuators	(1)	0.2554	0.2978	100.56	144.38	21.77
	(2)	0.6031	0.6803	33.17		
three actuators	(1)	0.2387	0.2762	94.25	165.90	24.55
	(2)	0.5036	0.6353	32.14		
	(3)	0.7701	0.4044	6.70		
three actuators (Lab)	(1)	0.167	0.5	39.81	25.43	19.95
	(2)	0.5	0.833	98.24		
	(3)	0.833	0.167	122.64		

Table 6. Typical example of CPU time for optimization

case	number of iteration	CPU time(sec)	percentage of main program (%) step 1,2	step 3	step 4	percentage of optimization program (%) step 1,2	step 3	step 4
one actuator	7	181	10.21	28.45	0.004	26.41	73.57	0.01
two actuators	27	2787	17.52	65.25	0.003	21.17	78.83	0.003
three actuators	7	2285	4.79	57.24	0.001	7.72	92.28	0.002

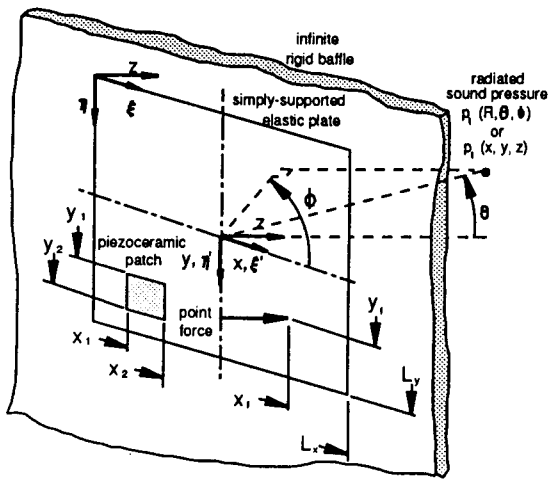

Figure 1. The arrangement and coordinates of the baffled simply-supported plate

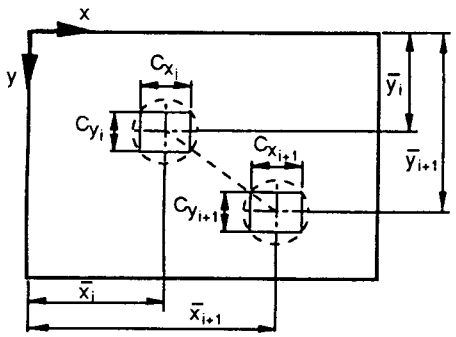

Figure 2. Illustration of design variables

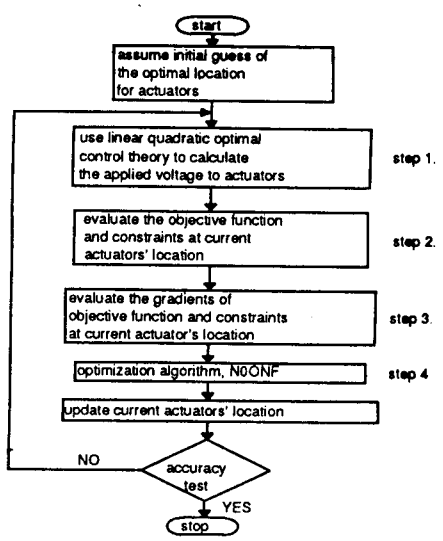

Figure 3. Flow chart of solution strategy

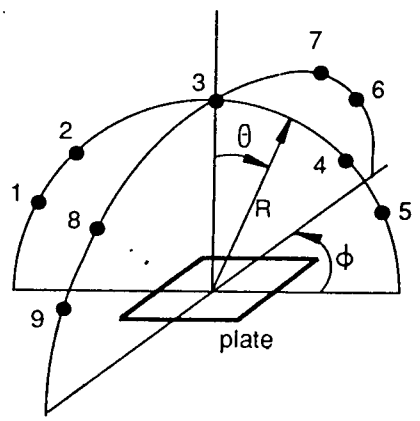

Figure 4. Location of error microphones

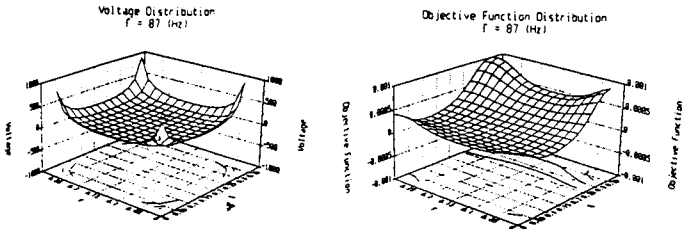

Figure 5. Distribution of objective function and control voltage for f=87 Hz

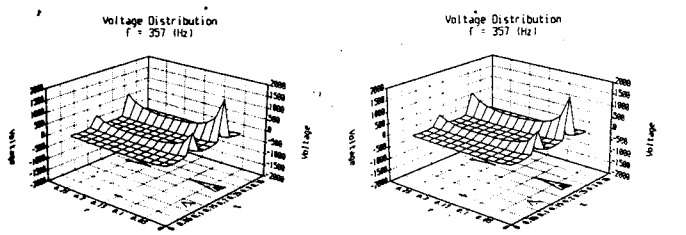

Figure 6. Distribution of objective function and control voltage for f=357 Hz

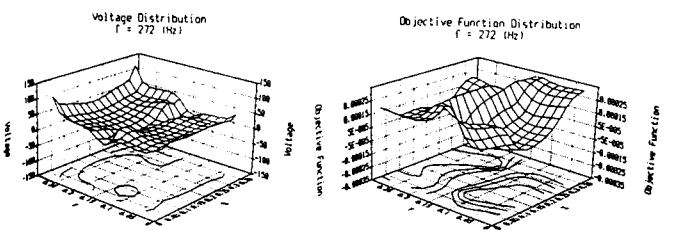

Figure 7. Distribution of objective function and control voltage for f=272 Hz

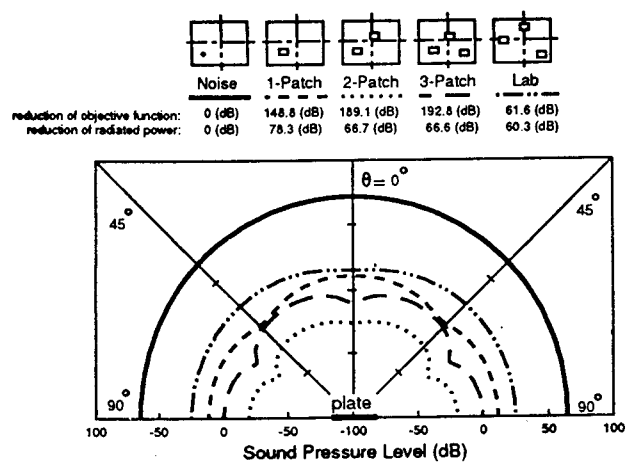

Figure 8. Radiation directivity pattern for f=357 Hz

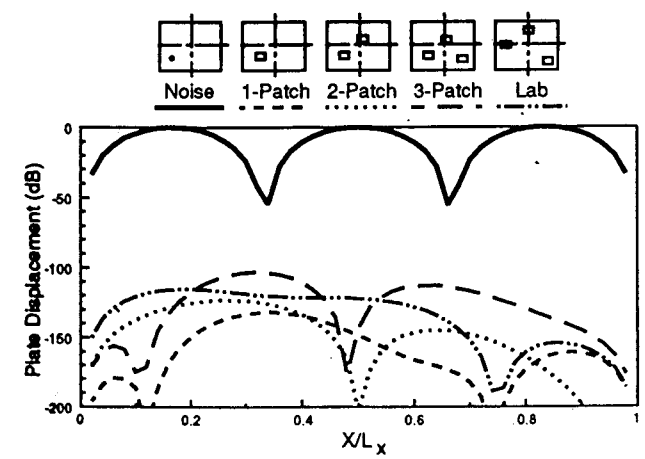

Figure 9. Plate displacement distribution for F=357 Hz

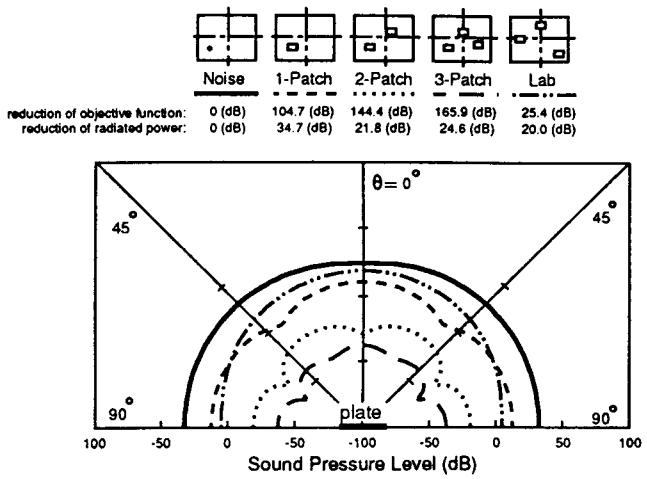

Figure 10. Radiation directivity pattern for f=272 Hz

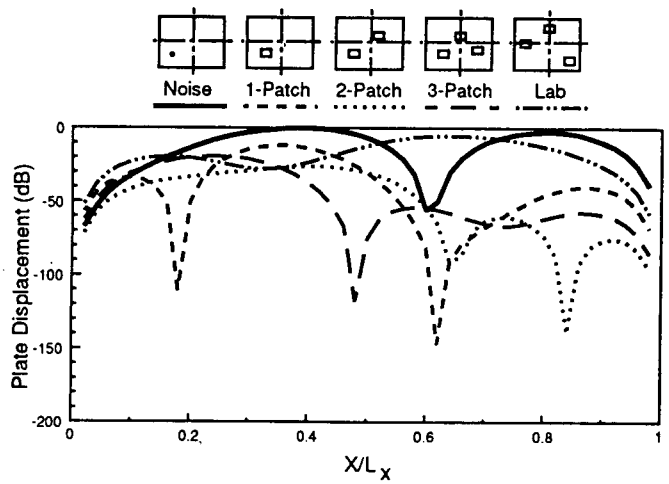

Figure 11. Plate displacement distribution for f=272 Hz

王栢村
國立屏東技術學院
機械工程技術系

Ricardo A. Budisso
Chris R. Fuller
維吉尼亞理工暨州立大學
機械工程系

摘　要

本篇論文提出壓電驅動器在最小平方控制系統之最佳化設計分析，目標函數、設計變數及限制區間均分別討論，舉一實例應用多個壓電驅動器在聲音幅射控制之位置最佳化選擇，應用線性平方最佳控制理論計算壓電驅動器之輸入電壓，再擷取壓電驅動器最佳位置使得目標函數爲最小值，此目標函數則爲由一串麥克風測得之聲壓最小平方和，可求得驅電驅動器之最佳位置，並證明與激振頻率有關，在共振與偏振激振之多個壓電驅動器之最佳位置均分別討論，結果顯示最佳化放置之壓電驅動器比任意放置的聲音幅射控制效果好，本研究提供了結合驅動器與感應器之智慧型材料結構系統的設計方法，經由最佳化設計也可適當減少控制驅動器之數量。